

THE UNUSUAL BINARY PULSAR PSR J1744–3922: RADIO FLUX VARIABILITY, NEAR-INFRARED OBSERVATION AND EVOLUTION

R. P. BRETON¹, M. S. E. ROBERTS², S. M. RANSOM³, V. M. KASPI¹, M. DURANT⁴, P. BERGERON⁵ AND A. J. FAULKNER⁶

Accepted for publication in ApJ, 2007 February 13

ABSTRACT

PSR J1744–3922 is a binary pulsar exhibiting highly variable pulsed radio emission. We report on a statistical multi-frequency study of the pulsed radio flux variability which suggests that this phenomenon is extrinsic to the pulsar and possibly tied to the companion, although not strongly correlated with orbital phase. The pulsar has an unusual combination of characteristics compared to typical recycled pulsars: a long spin period (172 ms); a relatively high magnetic field strength (1.7×10^{10} G); a very circular, compact orbit of 4.6 hours; and a low-mass companion ($0.08 M_{\odot}$). These spin and orbital properties are likely inconsistent with standard evolutionary models. We find similarities between the properties of the PSR J1744–3922 system and those of several other known binary pulsar systems, motivating the identification of a new class of binary pulsars. We suggest that this new class could result from either: a standard accretion scenario of a magnetar or a high-magnetic field pulsar; common envelope evolution with a low-mass star and a neutron star, similar to what is expected for ultra-compact X-ray binaries; or, accretion induced collapse of a white dwarf. We also report the detection of a possible $K' = 19.30(15)$ infrared counterpart at the position of the pulsar, which is relatively bright if the companion is a helium white dwarf at the nominal distance, and discuss its implications for the pulsar’s companion and evolutionary history.

Subject headings: binaries: pulsars: individual (PSR J1744–3922) — binaries: pulsars: evolution (PSR J1744–3922)

1. INTRODUCTION

A mid-Galactic latitude pulsar survey with the Parkes Radio Telescope (Crawford et al. 2006) detected three new pulsars in binary systems, none of which easily fits within the standard evolutionary scenarios proposed for the majority of recycled pulsars. One of them, PSR J1744–3922, was independently discovered during the reprocessing of the Parkes Multibeam Pulsar Survey data (Faulkner et al. 2004). This 172-ms binary pulsar has a relatively high surface dipole magnetic field strength ($B \equiv 3.2 \times 10^{19} (P\dot{P})^{1/2} \text{ G} = 1.7 \times 10^{10} \text{ G}$) suggesting it is mildly recycled. However, it appears to have a very light companion (minimum mass $0.085 M_{\odot}$) in a tight and nearly circular 4.6-hr orbit (see Table 1). This type of orbit and companion are typical of those of fully recycled pulsars (which we define as pulsars with $P \lesssim 8$ ms and $B \lesssim 10^9$ G) with He white dwarf (WD) companions. Thus, why PSR J1744–3922 escaped being fully recycled is a puzzle.

In addition to this atypical combination of spin and orbital properties, PSR J1744–3922 exhibits strong pulsed radio flux modulations, making the pulsar undetectable

at 1400 MHz for lengths of time ranging from a few tens of seconds to tens of minutes. It has been suggested by Faulkner et al. (2004) that this behavior might be the nulling phenomenon seen in a handful of slow, isolated pulsars. Nulling is a broad-band, if not total, interruption of the radio emission for a temporary period of time. On the other hand, although nulling could affect pulsars in binary systems as well, many binary pulsars vary due to external effects such as eclipses. Such external effects might explain PSR J1744–3922’s variability as well.

In this paper, we first report on multi-frequency observations of this pulsar that suggest the radio variability is not intrinsic to the pulsar. However, our analysis does not show strong evidence of a correlation between radio flux and orbital phase, as one might expect from traditional eclipse-like variability. We then report on our infrared search for a counterpart of the companion using the Canada-France-Hawaii Telescope (CFHT). This observation has identified a $K' = 19.30(15)$ star at the position determined by the radio timing observations. Finally, we examine why other properties of this pulsar make it incompatible with standard evolutionary scenarios, and identify a few other systems which have similar characteristics. The addition of PSR J1744–3922 as an extreme case among this group motivates us to identify a possible new class of binary pulsars. We propose several possible evolutionary channels which might produce members of this class and explain how the nature of the companion to PSR J1744–3922 could be used to constrain the origin of these systems.

2. PULSED RADIO FLUX VARIABILITY

The observed average pulsed radio emission from a pulsar can fluctuate for several different reasons. These include effects from the pulsar itself, as in nulling

arXiv:astro-ph/0702347v1 13 Feb 2007

¹ Department of Physics, Rutherford Physics Building, McGill University, Montreal, QC H3A 2T8, Canada; bretonr@physics.mcgill.ca

² Eureka Scientific, Inc., 2452 Delmer Street Suite 100 Oakland, CA 94602-3017

³ National Radio Astronomy Observatory, 520 Edgemont Road, Charlottesville, VA 22903

⁴ Department of Astronomy and Astrophysics, University of Toronto, 60 St. George Street, Toronto, ON M5S 3H8, Canada

⁵ Département de Physique, Université de Montréal, C.P. 6128, Succ. Centre-Ville, Montréal, QC H3C 3J7, Canada

⁶ University of Manchester, Jodrell Bank Observatory, Macclesfield, Cheshire, UK SK11 9DL

(e.g. Backer 1970), its environment, as in eclipsing binary pulsars (e.g. Fruchter, Stinebring & Taylor 1988), or the interstellar medium, as in scintillation (e.g. Rickett 1970). In the case of PSR J1744–3922, during a typical 1400 MHz observation, the radio emission seems to turn on and off randomly on timescales varying from tens of seconds to tens of minutes (see Figure 1 for sample folded profiles). In many instances, the pulsar is undetectable through entire observations (~ 15 min). In a previous analysis of these radio flux modulations, Faulkner et al. (2004) concluded on the basis of observations at 1400 MHz that PSR J1744–3922 is probably a pulsar experiencing pulse nulls. As nulling is a broadband phenomenon (e.g. Bartel et al. 1981), we decided to investigate the frequency dependence of the fluctuations in order to test the nulling hypothesis.

2.1. Data and Procedure

The work we report is based on an extended dataset combining both the data reported independently by Faulkner et al. (2004) and by Ransom et al. (in prep.). A total of 112 radio timing observations of PSR J1744–3922 were made at the 64-meter Parkes Telescope and the 100-meter Green Bank Telescope between 2003 June and 2006 January. Relevant details for the current study are summarized in Table 2 and we refer to the above two papers for more details about the observational setups and timing results.

For the purpose of studying the radio emission variability, we made time series of the pulsed flux intensity. We dedispersed the data at the pulsar’s dispersion measure (DM) of 148.5 pc cm^{-3} and then folded the resulting time series in 10-s intervals using the timing ephemerides from Ransom et al. (in prep.). For each observation, the pulse phase was determined from the profile averaged over the entire observation. We fit each 10-s interval of the folded pulse profile with a constant baseline plus a Gaussian of variable amplitude having a fixed width at the predetermined phase. A Gaussian $\text{FWHM} = 0.01964P$, where P is the pulse period, nicely fits the profile averaged over many observations in the frequency range 680–4600 MHz. Errors on the best-fit amplitudes returned by our least-square minimization procedure were scaled under the assumption that the off-pulse region RMS represents the total system noise. Although no flux standard has been observed, we obtained pulsed flux density estimates by using the radiometer equation and equating predicted noise levels to the off-pulse RMS level. We also accounted for the offset between the telescope pointing and the real position of the source (since in the early observations the best-fit timing position had not yet been determined) by approximating the telescope sensitivity to be an azimuthally symmetric Gaussian having a FWHM corresponding to the radio telescope beam size, which is $8.8'$ and $13.8'$ at 1400 MHz for GBT and Parkes, respectively.

In this way, we generated flux time series for all 112 observations of PSR J1744–3922 (see Figure 2 for examples). As we describe next, these results show that scintillation and nulling are highly unlikely to be the origin of the observed variability.

2.2. Radio-frequency-dependent Variability

As Faulkner et al. (2004) discussed previously, interstellar scintillation (ISS) is unlikely to be the source of

fluctuations in PSR J1744–3922. Scintillation is produced by a diffractive scattering medium along our line of sight and the typical diffractive scintillation timescale can be expressed as (see Cordes & Rickett 1998):

$$\Delta t_d = 2.53 \times 10^4 \frac{D \Delta \nu_d}{\nu V_{ISS}} \text{ s}, \quad (1)$$

with D the distance to the source in kpc, $\Delta \nu_d$ the decorrelation bandwidth in MHz, ν the observed frequency in GHz and V_{ISS} the velocity of ISS diffraction pattern in km s^{-1} . For the 1400 MHz observation shown in Figure 1, for example, the NE2001 model for the Galactic distribution of free electrons (Cordes & Lazio 2002) predicts $\Delta \nu_d = 0.01$ MHz in the line of sight of PSR J1744–3922 at a distance of 3.0 kpc estimated from the DM. V_{ISS} is typically dominated by the pulsar velocities, which are in the range 10 – 100 km s^{-1} for most binaries. Therefore, we estimate the scintillation timescale to be of the order of a few seconds to a minute at most. This could be compatible with the fast flux variations but can certainly not explain the extended periods where the pulsar goes undetected. Perhaps most importantly, strong scintillations will be averaged away since typical observing bandwidths are much larger than the decorrelation bandwidth, and therefore contain many “scintles”. Such averaging effectively rules out the ISS hypothesis.

Another possibility is that the flux modulation is related to intrinsic nulling of the pulsar. Based on observations at 1400 MHz only, Faulkner et al. (2004) identified it as the most likely explanation. Only observed in old, isolated pulsars so far, (though nothing prevents a binary pulsar from being a nuller) nulling is a broad-band, if not total, interruption of the radio emission (e.g. Bartel et al. 1981).

Considering the fraction of observations with no detection of radio emission at various frequencies (see Table 3), we note qualitatively that PSR J1744–3922 is regularly undetectable at low frequencies but easily detectable at high. For instance, we obtained four Parkes observations at 680 and 2900 MHz simultaneously in which the pulsar is detected twice at 2900 MHz while remaining undetected at 680 MHz. In addition, seven long GBT observations centered at 1850 and 1950 MHz show highly variable emission but little evidence that the pulsar ever disappears completely (see Figure 2). Clearly, however, observations could be biased by the relative instrumental sensitivity in each band and by the intrinsic spectrum of the pulsar.

To investigate the effect of instrumental sensitivity and spectral energy distribution, we analysed the pulsed flux densities at different frequencies. Measured values were estimated using the radiometer equation as explained in Section 2.1 and are displayed in Table 4. We note that Faulkner et al. (2004) reported a different flux density than ours at 1400 MHz ($0.20(3)$ vs. $0.11(3)$ mJy, respectively). The discrepancy could be because the average flux density changes depending on the amount of time PSR J1744–3922 spends in its “bright state” during an observation. The large standard deviation (0.16 mJy, see Table 4) at this frequency suggests that by restricting the calculation to observations for which PSR J1744–3922 is nicely detected, a higher flux value can be obtained.

For the simultaneous observations at 680 and

2900 MHz in which the pulsar was not detected at 680 MHz (see Table 2), we can put an interesting approximate lower limit on the spectral index, α , of the pulsar if we assume that the minimum detectable pulsed flux at 680 MHz is an upper limit to the pulsed flux at this frequency:

$$\alpha \gtrsim \frac{\log(S_{2900}/S_{680})}{\log(\nu_{2900}/\nu_{680})} \simeq 0.17. \quad (2)$$

Such a value is extremely flat compared to that of the average population of pulsars, which has a spectral index of -1.8 ± 0.2 (Maron et al. 2000). Thus either PSR J1744–3922 has a spectrum very different from those of most pulsars and/or the flux variability is intrinsically frequency dependent.

The distribution of pulsed flux density values for all 1400 and 1950 MHz observations is shown in Figure 3. It is clear from the distribution at 1400 MHz that the numerous non-detections are responsible for the peak below the sensitivity threshold. We also observe that the 1400 MHz flux density has a higher average value and is much more variable than at 1950 MHz. This frequency dependence suggests some sort of scattering mechanism with the unscattered flux level much higher than the observed average flux at 1400 MHz, and argues against it being classical nulling. Therefore, we conclude that this unknown mechanism affecting the lower frequency flux might be responsible for the apparent flat spectrum derived from the simultaneous 680–2900 MHz observation.

Recent simultaneous multi-frequency observations of PSR B1133+16, a well-established nuller, show that single pulse nulls do not always happen simultaneously at all frequencies (Bhat et al. 2006). They also observe, however, that the overall null fraction does not present any evidence of frequency dependence, which might mean that sometimes nulls are simply delayed at some frequencies. In the case of PSR J1744–3922, the S/N limits us to consider the pulsed flux over times corresponding to many pulse periods only. Therefore, the kind of non-simultaneous, frequency-dependent effect seen by Bhat et al. (2006) is not relevant to our analysis and thus we expect the variability to be independent of frequency if really caused by nulling.

Although our flux measurements at other frequencies are not simultaneous, we can assume they are good statistical estimates of the normal flux of the pulsar and use them to characterize its spectrum. In an attempt to estimate an unbiased spectral index, we can use the approximate maximum flux value at each frequency. The 1400, 1850, 1950, 2900 and 4600 MHz data give a spectral index lying between -1.5 and -3.0 , which is similar to many known pulsars. However, it seems that the flux at 820 MHz is much smaller than expected from a single power-law spectrum. Since flux variations are very important at low frequency and we only have a single detection at 820 MHz, the reported maximum value is probably not representative of the real flux of the pulsar at this frequency.

In summary, the facts that the pulsar radio emission rarely drops below our detection threshold at 1950 MHz and that the radio variability is frequency dependent, demonstrate that the flux modulation is probably not classical nulling. A non-nulling origin for the fluctuations

at 1400 MHz also explains why PSR J1744–3922 does not fit in with expectations based on the correlations observed between null fraction and spin period (Biggs 1992), and between null fraction and equivalent pulse width (Li & Wang 1995). In comparison with nullers, it has one of the smallest spin periods and a small pulse width (~ 3.4 ms), but one of the largest “null” fractions ($\sim 60\%$ at 1400 MHz). Since this pulsar is in a tight binary system, the possibility of influence by its companion is therefore an important alternative to consider.

2.3. Orbital Correlation Analysis

Even though a quick examination of the time series confirms that the flux decreases observed for PSR J1744–3922 are not due to systematic eclipses of the pulsar by its companion, a more subtle orbital correlation could exist. To search for such an effect, we ask whether or not the pulsar is more likely to be detected at a particular orbital phase. For this analysis, we folded the time series in 1-min intervals, and defined the pulse as detected if the best-fit Gaussian amplitude was greater than its 1σ uncertainty. In order to limit spectral effects, we restrict the analysis to observations covering the range 1237.5–1516.5 MHz at Parkes⁷ and 1404.5–1497.5 MHz at GBT.

The results of this analysis are shown in Figure 4a. The histogram represents the fraction of detected pulses with respect to the total number observed, as a function of orbital phase. Errors were determined using Poisson statistics, implicitly assuming our assigning of each interval as a detection or non-detection is accurate. There is a suggestion that PSR J1744–3922 is more often undetectable between phases $\sim 0.05 - 0.45$. The best-fit constant model gives a $\chi^2/9 = 5.85$ (the histogram has 10 orbital phase bins), which, if correct, would be highly significant. To test the accuracy of our errors, we performed a Monte Carlo simulation consisting of 10000 trials where we assigned each measurement a random orbital phase. The mean $\chi^2/9 = 0.37$ with a standard deviation of 0.18, suggesting our error estimates are significantly overestimated.

To investigate further, we performed an analysis similar to the previous one but for the pulsed flux density measured at each orbital phase averaged over all observations. We selected two subsets of data: the Parkes and GBT observations made at 1400 MHz and the GBT 1950 MHz observations. The first one includes 101 observations which are on average ~ 15 minutes long, but there are a few observations which are significantly longer. The latter subset includes four observations, two of which have full orbital coverage, one covering $\sim 75\%$ of the orbit and the last one $\sim 40\%$. Observations with no detection of PSR J1744–3922 are assigned upper limit values of three times the background noise level (which is very small compared with the average pulse of the pulsar when it is on). Errors in each bin of the histogram are estimated from the RMS of the individual values in each orbital bin. Results are plotted in Figure 4b. For the 1400 MHz data, a fit to a constant line has a $\chi^2/9 = 15.58$, and for the GBT 1950 MHz data, we find a $\chi^2/9 = 5.59$. Randomizing the individual data

⁷ This is the common range of the observing modes centered at 1375 and 1400 MHz.

points and folding them resulted in a $\chi^2/9 = 1.02$ at both frequencies, suggesting our error estimates are reasonable. Although this analysis strongly rules out the constant model for our folded light curves, the shapes of these curves at 1400 and 1950 MHz are not consistent with each other.

This could be a result of the paucity of observations (typically 3–5) at any given orbital phase. Therefore, random fluctuations in the flux on timescales of tens of minutes (which we see in the time series) would likely not be averaged out. To test whether or not the significant deviation from a constant model depends on the particular phasing of our observations, we again performed Monte Carlo simulations in which 10000 trial histograms similar to those shown in Figure 4 were generated from the real data by adding a random orbital phase shift at the beginning of each time series and then determining the $\chi^2/9$ value for a constant model. From the resulting distribution of $\chi^2/9$ values, we estimate the chance probability of obtaining the particular $\chi^2/9$ values obtained, or higher, using the real orbital phases. For the on-off analysis, the probability is 0.102, or a formal $\chi^2/9 = 1.63$. For the 1400 and 1950 MHz flux density light curves, the probabilities are 0.015 ($\chi^2/9 = 2.28$) and 0.212 ($\chi^2/9 = 1.34$). This suggests there may be some correlation with the orbit, but the shape of our folded light curves are still dominated by more stochastic flux variations given our limited data set. We would expect a standard eclipse mechanism to make the pulsar dimmer when the companion is in front of it at phase 0.25, which does not seem to be the case. There may be large orbit to orbit variations in the eclipse depths, durations, and phases. This kind of behavior has been observed in other binary pulsar systems such as Ter5A, Ter5P, Ter5ad and NGC6397A (see Ransom et al. 2005; Hessels et al. 2006; D’Amico et al. 2001, for examples), but a much larger data set would be required to obtain a reliable average light curve to show if this is the case for PSR J1744–3922. It is still possible that the short time scale pulsed flux variations tend to group in “events” during which the pulse gets dimmer. These “events” may last for a significant fraction of the orbital phase causing the apparent marginal orbital correlation given our limited statistics.

2.4. Accretion and mass loss limits

Many other systems are known to exhibit strong flux radio variations for which the orbital dependence is well established. One of them is PSR B1718–19 (Lyne et al. 1993). Interestingly, this pulsar has a low-mass companion and orbital properties similar to those of PSR J1744–3922 and is also harder to detect at low frequency. At 408 and 606 MHz, PSR B1718–19 gets so dim that it is barely detectable in spite of good sensitivity during a large part of the orbit. On the other hand, at 1404 and 1660 MHz the orbital modulation of the average flux is much less important. This flickering is probably made by material left over by the wind of the companion, a bloated main sequence (MS) star (Janssen & van Kerkwijk 2005). Although the companion of PSR B1718–19 is not large enough to come near to filling its Roche-lobe, this could happen in a tighter binary system like that of PSR J1744–3922. In this

case, some kind of tidal stripping could be occurring, leaving material around the system. This could explain why the pulsar does not disappear at conjunction like PSR B1718–19 does, but in a more stochastic way.

If the companion is losing mass, one might expect to observe small changes in the orbital parameters. From radio timing (see Ransom et al. in prep.), we can set an upper limit of $|\dot{P}_{orb}| < 2 \times 10^{-10} \text{ s s}^{-1}$ and $|\dot{x}| < 7 \times 10^{-12} \text{ lt-s s}^{-1}$ on the rate of change of the orbital period and the rate of change of the projected semi-major axis, respectively. We can use the latter quantity to evaluate the implied mass loss limit. For a circular orbit, which is a good approximation here, we can express the rate of change of the semi-major axis as (Verbunt 1993):

$$\frac{\dot{a}}{a} = 2 \frac{\dot{J}}{J} - 2 \frac{\dot{M}_c}{M_c} \left(1 - \frac{\beta M_c}{M_p} - \frac{(1-\beta)M_c}{2(M_p + M_c)} - \alpha(1-\beta) \frac{M_p}{M_p + M_c} \right), \quad (3)$$

where $x = a \sin i$, $\dot{x} = \dot{a} \sin i$, M_c and M_p are the mass of the companion and the pulsar, respectively, J is the total angular momentum of the system, β is the fraction of mass accreted by the pulsar and α is the specific angular momentum of the mass lost in units of the companion star’s specific angular momentum.

For the case in which the total orbital angular momentum of the system is preserved ($\dot{J} = 0$) we can see that mass loss from the companion⁸ ($\dot{M}_c < 0$) would necessarily lead to a widening ($\dot{a}/a > 0$) of the orbit if: 1) the mass transfer is conservative ($\beta = 1$), or 2) the mass transfer is non-conservative ($\beta < 1$) and $\alpha < 1 + M_c/(2M_p)$ (see Verbunt 1993, for more details).

By considering the conservative case, in which $|\dot{M}_c| = |\dot{M}_p|$, we obtain an upper limit on a possible mass accretion rate by the pulsar $|\dot{M}_p| \lesssim 3 \times 10^{-12} M_\odot \text{ yr}^{-1}$. This would be even lower for the non-conservative case. Accretion onto the pulsar is possible if the corotation radius:

$$r_{co} \simeq 500 P_{\text{psr}}^{2/3} M_{1.4}^{1/3} \text{ km}, \quad (4)$$

is larger than the magnetospheric radius of the pulsar:

$$r_{mag} \simeq 800 \left(\frac{B_{\text{psr}}^4 R_{10}^{12}}{M_{1.4} \dot{M}_{-12}^2} \right)^{1/7} \text{ km}, \quad (5)$$

where P_{psr} and B_{psr} are, respectively, the spin period and the surface dipole magnetic field in units of PSR J1744–3922’s P and B (172 ms and $1.68 \times 10^{10} \text{ G}$); $M_{1.4}$ is the mass of the pulsar in units of $1.4 M_\odot$; R_{10} is the radius of the pulsar in units of 10 km; and \dot{M}_{-12} is the accretion rate in units of $10^{-12} M_\odot \text{ yr}^{-1}$. Given the upper limit on the mass accretion rate, and the likely conservative $R_{10} = 1$ value for the neutron star radius, we find that r_{mag} ($\gtrsim 600 \text{ km}$) is likely larger than r_{co} ($\sim 500 \text{ km}$). This argues against any significant accretion occurring in the system.

That no significant accretion is occurring is also supported by an XMM-Newton observation that allows Ransom et al. (in prep.) to put a conservative upper

⁸ Here we implicitly assume that $M_c < M_p$.

limit $\sim 2 \times 10^{31} \text{ erg s}^{-1}$ on the unabsorbed X-ray flux from accretion in the 0.1-10 keV range. Assuming

$$L_X = \frac{\eta G M \dot{M}}{R}, \quad (6)$$

with a conversion efficiency of accretion energy into observed X-rays $\eta = 0.1$, we get $\dot{M}_p \lesssim 2 \times 10^{-14} M_\odot \text{ yr}^{-1}$ for accretion at the surface of the pulsar and $\dot{M}_p \lesssim 2.4 \times 10^{-12} M_\odot \text{ yr}^{-1}$ if accretion is limited to the boundary of the magnetospheric radius. Therefore, it appears unlikely that PSR J1744–3922 is accreting and, if the companion is losing mass, it is probably expelled away from the system.

3. INFRARED OBSERVATIONS

The radio flux variability, which might be due to material leaving the surface of the companion, and the atypical evolutionary characteristics of the pulsar (see Section 4) can be investigated further by observing its companion at optical or near-infrared wavelengths. We imaged the field of PSR J1744–3922 at K' -band on the night of 2005 April 19 using the Canada-France-Hawaii 3.6-m Telescope (CFHT) at Mauna Kea. The telescope is equipped with the Adaptive Optic Bonnette (AOB, Rigaut et al. 1998), which provides good correction for atmospheric seeing, and KIR, the 1024×1024 pixel HAWAII infrared detector with $0''.0348$ pixel scale. The total integration time was $30 \text{ s} \times 59 \text{ integrations} = 1770 \text{ s}$.

We subtracted a dark frame from each image, and then constructed a flat-field image from the median of the science frames. The images were then flat-fielded, registered and stacked to make the final image. The final stellar profile has a FWHM of $0''.17$, degraded somewhat from the optimal correction provided by the AOB system due to a high airmass (~ 2.0) and poor natural seeing. Figure 5 shows the final image we obtained.

We analyzed the final CFHT image using the standard routine `daophot` (Stetson 1987) for PSF fitting photometry, and calibrated the image using the standard star FS34 (Casali & Hawarden 1992). To find the photometric zero point, we performed photometry on the standard star with a large aperture containing most of the flux, and applied an aperture correction for the PSF stars in the science image. Careful calibration of measurement errors has been done by adding artificial stars of known magnitude to blank parts of the image and then measuring their magnitude through the PSF fitting process along with the real stars. Thus, errors on the magnitude returned by `daophot` can be rescaled by calculating the standard deviation for the added stars.

We found the astrometric solution for the image by cross-identifying five stars with the 2MASS catalogue (Skrutskie et al. 2006), fitting for scale, rotation and displacement. The final astrometric uncertainty is $0''.34$ at the 3σ confidence level. This value depends on the matching to the reference stars because the error on the radio timing position of PSR J1744–3922 is negligible, ($\sim 0''.03$). The final image is displayed in Figure 5, with the positional error circle centered at the radio position of PSR J1744–3922: $\alpha = 17^{\text{h}}44^{\text{m}}02^{\text{s}}.667(1)$ and $\delta = -39^{\circ}22'21''.52(5)$. Only one star falls inside this circle, and for this we measure $K' = 19.30(15)$. We observe that, above the 3σ detection limit, the average stellar

density is $0.079 \text{ arcsec}^{-2}$ and hence the probability of a star falling in the error circle is only 2.9%. Due to its positional coincidence and the low probability of chance superposition, we henceforth refer to this object as the possible counterpart to PSR J1744–3922.

Unfortunately our near-infrared observation does not tightly constrain the nature of the companion to PSR J1744–3922, mainly because of the uncertainties in the distance to the system and in the companion mass, as well as the fact that its temperature is unknown. Assuming the NE2001 (Cordes & Lazio 2002) electron density model is correct, we infer a DM distance of $3.0 \pm 0.6 \text{ kpc}$ and hence a distance modulus ranging from 11.9 to 12.8. Using the three-dimensional Galactic extinction model of Drimmel et al. (2003) we get a value of $A_V \simeq 1.9$ for a distance of 3.0 kpc. Converting⁹ the inferred extinction to K' band gives $A_{K'} \simeq 0.21$ (see Rieke & Lebofsky 1985, for conversion factors). Therefore the estimated absolute magnitude of the counterpart lies in the range $M_{K'} \simeq [6.1, 7.4]$.

We can evaluate how probable it is that the companion is a He WD, a typical low-mass companion in binary pulsar systems, since WD cooling models can put restrictions on the stellar mass and cooling age, given an observed flux. Figure 6 shows the absolute K' magnitude as a function of cooling age for He WDs of different masses. These cooling tracks were made by using WD atmosphere models based on the calculations of Bergeron et al. (1995), and thereafter improved by Bergeron et al. (2001) and Bergeron (2001), in combination with evolution sequences calculated by Driebe et al. (1999). Although the mass range of models available to us does not go below $0.179 M_\odot$, we can deduce that to be so luminous, a He WD would need to have a very low mass and a cooling age much lower than the characteristic age of the pulsar (1.7 Gyr). Even if the mass were equal to the lower limit of $0.08 M_\odot$ derived from radio timing, it seems unlikely that such a companion could be as old as the pulsar characteristic age. Therefore, if the companion is indeed a He WD, the pulsar’s spin period must be close to the equilibrium spin frequency it reached at the end of the recycling process. In this case, its characteristic age is an overestimate of its true age.

Another possibility is that the companion is not a He WD. If the companion is a low-mass main sequence (MS) star, then the minimum mass required to match the lower limit on the absolute K' flux is $\sim 0.25 M_\odot$, regardless of the pulsar age. Such a companion mass requires a favorable face-on orbit but this cannot be ruled out from the near-infrared and radio data. On the other hand, a lower-mass bloated MS star could be equally as bright, so is also a possibility.

We cannot constrain the nature of the counterpart very well from a measurement in a single near-infrared filter. Ideally, obtaining a spectrum could yield: 1) a precise determination of the nature of the counterpart, 2) orbital Doppler shift measurements of the spectral lines which can prove the association as well as determine the mass ratio, 3) in the case of a white dwarf, an estimate of its cooling age from spectral line fitting.

⁹ For simplicity, and because the error on the magnitude is dominated by the distance estimate, we hereafter assume that K and K' are similar.

4. BINARY PULSAR EVOLUTION

The sporadic radio emission from PSR J1744–3922 is not the only indication that there is something unusual about the pulsar’s interaction with its companion. The pulsar is in a tight and low eccentricity ($e < 0.001$) orbit with an apparently very light companion having a minimum mass of $0.08 M_{\odot}$. On the other hand it has a relatively large surface magnetic field (1.7×10^{10} G) and an extremely long spin period (172 ms) compared with other binary pulsars having low-mass companions (see, e.g., Stairs 2004; van Kerkwijk et al. 2004, for recent reviews). These properties, along with the relatively bright near-infrared counterpart of the companion, make it unusual and suggest it evolved differently than most binary pulsars.

In binary pulsar evolution, the nature of the companion plays a key role in determining the final spin and orbital characteristics of the system. Most of the binary pulsar population consists of pulsars with low-mass companions in low-eccentricity orbits. Following the nomenclature adopted by Stairs (2004), the *case A* evolutionary channel results in pulsars having He WD companions. They are neutron stars (NS) which were spun up to very short periods ($P \lesssim 8$ ms) after accreting matter from a low-mass star during a long and steady Roche-lobe overflow (RLO) phase (Tauris & Savonije 1999). For reasons that are not yet understood, this process is responsible for the partial suppression of the surface magnetic field to values of the order of 10^{8-9} G. The most robust predictions of this model are the correlations linking the orbital period to the mass of the He WD (Rappaport et al. 1995) (see Figure 7) and the eccentricity to the orbital period (Phinney 1992).

On the other hand, the *case B* channel is made of pulsars having more massive CO WD or ONeMg WD companions ($M_c \gtrsim 0.45 M_{\odot}$). Their intermediate mass progenitors did not sustain a stable RLO phase, instead evolving in a short-duration, non-conservative, common envelope (CE) phase during which the pulsar spiraled into its companion’s envelope. This process only partly recycled the pulsar, leading to intermediate spin periods ($P \gtrsim 8$ ms) and leaving a higher magnetic field ($\sim 10^9-10^{10}$ G).

In Table 5, the expected properties of systems resulting from these two evolutionary channels are compared with those of PSR J1744–3922. Both scenarios fail to account for all the observed characteristics; this suggests a special evolution for PSR J1744–3922. This can also be seen from a P – B diagram (Figure 8a) made for binary pulsars in the Galactic field having circular orbits. As opposed to isolated and other kinds of non-recycled binary pulsars, there exists a very strong relationship linking P and B which is presumably related to the recycling process. To our knowledge, such a correlation has not been reported in the recent literature although was indirectly found by van den Heuvel & Bitzaraki (1995) who reported a possible correlation between $P - P_{orb}$ and $B - P_{orb}$ for binary pulsars in circular orbits. The many binary pulsars discovered in recent years may be making it easier to appreciate. In Figure 8a we see that pulsars having light companions (*case A*) generally gather in the region of low magnetic field and short spin period whereas the *case B* pulsars lie in higher-valued regions. Surprisingly,

of the six highest magnetic field pulsars, five of them, including PSR J1744–3922, have light companions. The remaining one, PSR B0655+64, is an extreme system associated with the *case B* channel since it has a massive WD companion (van Kerkwijk et al. 2004). However, the *case B* channel cannot accommodate the other five pulsars because, assuming random orbital inclinations, a simple statistical estimate gives less than a 0.1% probability for all of them to be more massive than the required $0.45 M_{\odot}$. For PSR J1744–3922 in particular, the orbital inclination would need to be less than 12.5° , which represents a 2.5% probability.

We *also* report in Table 5 the principal characteristics of binary pulsars that appear to be partly recycled (e.g. $P > 8$ ms and $e < 0.01$) but have companions likely not massive enough to be explained by the standard *case B* scenario. These pulsars have related properties and could have experienced similar evolutionary histories. Apart from their strange position in the $P - B$ diagram, they also stand out when we look at the $P_{orb} - P$ relationship (Figure 8b). In this plot, we see that pulsars having low-mass companions (*case A*) occupy the bottom region, below $P \lesssim 8$ ms, and their spin periods are more or less independent of the orbital period. This arises from the fact that recycling probably saturates for a given accretion rate and/or accretion mass (Konar & Choudhuri 2004). On the other hand, fewer constraints exist in this parameter space for pulsars with massive WD companions (*case B*). Their short CE evolution would limit the recycling efficiency and thus the final parameters are more sensitive to the initial conditions. Finally, we observe a third category made of relatively slow pulsars with low-mass companions in compact orbits. Neither the *case A* nor the *case B* scenarios is able to explain such properties, especially for the most extreme systems like PSR J1744–3922 and PSR B1831–00. Therefore, we suggest a new “class” of binary pulsars having the following properties: 1) long spin periods (in comparison to MSPs), 2) large surface magnetic fields ($\sim 10^{10-11}$ G), 3) low-mass companions, likely $0.08 - 0.3 M_{\odot}$, having nature yet to be determined, 4) low eccentricities, and possibly 5) short orbital periods ($\lesssim 5$ d). On this last point, very wide orbit systems like PSR B1800–27 and PSR J0407+1607 might be explained by the standard *case A* scenario in which it is difficult to achieve an extended period of mass transfer from the companion to the pulsar.

5. DISCUSSION

The existence of another “class” of binary pulsars is supported by the fact that several pulsars now occupy a region of the parameter space delimited by the spin period, orbital period, magnetic field and companion mass that seems inaccessible to the standard evolutionary channels. PSRs J1744–3922, J1232–6501, B1718–19 and B1831–00 are certainly the most noticeable candidates. Although other papers also identified that some of these pulsars have strange characteristics (see, e.g., van den Heuvel & Bitzaraki 1995; Sutantyo & Li 2000; Edwards & Bailes 2001), there is no consensus on their evolutionary histories. For instance the case of PSR B1718–19 was considered somewhat unique because it is in a globular cluster and hence has possibly been partly perturbed, or even greatly changed,

by stellar interactions (Ergma et al. 1996). The discovery of PSR J1744–3922, in the Galactic field, is important because it strengthens the possible connection between PSR B1718–19 and other similar binary pulsars in the field. Unless they do not have WD companions, these pulsars were at least partially recycled because tidal circularization is needed to explain eccentricities of 0.01 and smaller. However some of them have eccentricities $10^{-3} - 10^{-2}$, relatively large given their very short orbital periods, which is in contrast to tight *case A* systems having smaller eccentricity (Phinney 1992). In this section we speculate and put constraints on some scenarios that may explain this possible new class of pulsars.

5.1. Recycled High Magnetic Field Pulsar Channel

One possibility is that pulsars like PSR J1744–3922 may initially have had a magnetar-strength magnetic field ($B \sim 10^{14} - 10^{15}$ G). Such a pulsar could experience standard *case A* evolution involving conservative RLO but since the initial magnetic field is higher by 1–2 orders of magnitude, at the end of the recycling process, the field might be 10^{10-11} G instead, consistent with observations. Since the recycling mechanism appears to strongly correlate the final magnetic field with the final spin period, the pulsar would also have an unusually long spin period as well.

Whether this extrapolation to magnetars and high magnetic field pulsars is valid depends on accretion-induced decay models of the magnetic field strength. Among the proposed mechanisms is magnetic field burial, in which material accretes through the polar cap and, while piling up at the poles, exerts a latitudinal pressure gradient by trying to spread toward the equator. This effect tends to drag the field lines away from the poles, increasing the polar cap radius and decreasing the magnetic moment of the pulsar. Payne & Melatos (2004) show that the magnetic field would naturally “freeze” to a minimum stable strength once the amount of accreted mass exceeds some critical value, if the magnetospheric radius is comparable to the size of the neutron star. According to Payne (2005), this critical mass could reach up to $1 M_{\odot}$ for a 10^{15} G NS and hence magnetic field suppression would be difficult to achieve due to the large amount of accretion mass required. However, accounting for other effects like the natural decay of magnetic field due to X-ray emission and high-energy bursts (see Woods & Thompson 2006, for a review), might make a partially suppressed final magnetic field of 10^{10} G plausible.

A recycled high magnetic field pulsar is expected to leave a He WD companion and follow the companion mass-orbital period relationship as for the normal *case A* systems. PSR B1718–19 is excluded from this kind of evolution because its companion is a bloated MS star. All the other pulsars listed in Table 5 are potential members, albeit PSRs B1800–27 and J0407+1607 would need relatively face-on orbits ($i < 30$ and 24° , implying 13 and 9% probability for randomly oriented orbits, respectively) to match the $P_{orb} - M_c$ relationship (Fig. 7). Another interesting prediction of this scenario is that, because the recycling process can leave pulsars with relatively long spin periods, they might not be very different from the spin periods when accretion ceased. Thus, the real age

could be much lower than the timing-based characteristic age, and the WD companions would have younger cooling ages as well.

The fraction of Galactic field binary pulsars in this class ($\sim 7/60$) might naively be thought to be similar to the fraction of observed magnetars with respect to the ordinary pulsars ($\sim 10/1500$). However, the observed population of magnetars suffers from severe selection effects because many of them appear to lie dormant, becoming observable for only brief intervals, like XTE J1810–197 (Ibrahim et al. 2004). Therefore, we can relate these parameters as follows:

$$\frac{N_{\text{class}}}{N_{\text{binary}}} = \frac{N_{\text{obs. mag.}}}{N_{\text{radio}}} \frac{1}{f_{\text{quies}}}, \quad (7)$$

where N_{class} is the number of pulsars in the new class, N_{binary} is the number of binary pulsar systems, $N_{\text{obs. mag.}}$ is the number of observed magnetars, N_{radio} is the number of radio pulsars and f_{quies} the fraction of magnetars in quiescence.

Hence we estimate that, due to quiescence, the fraction of observed magnetars with respect to the total population is about $\frac{10}{1500} / \frac{7}{60} \sim 0.06$. This would make a total population of ~ 175 magnetars which is consistent with the possible ~ 100 in our Galaxy estimated by Woods & Thompson (2006), who used $f_{\text{quies}} = 0.1$. Our crude calculation has many caveats: Is the binary magnetar population similar to the binary radio pulsar population? Can the short lifetime of magnetars and high magnetic field neutron stars limit the number of such recycled systems? Clearly, this latter point depends strongly on the time evolution of the self-induced decay of the magnetic field, which seems to operate on a time scale of a few tens of thousands of years (Kaspi 2004).

5.2. UCXB Evolutionary Track Channel

There exists a class of neutron stars and CO/ONeMg WDs that accrete from light He WD donors in ultra tight (few tens of minutes) orbits. These X-ray emitters, known as ultracompact X-ray binaries (UCXBs), may be the result of wider ~ 0.5 -day systems that have decayed due to gravitational wave radiation. A CE scenario has been proposed as a viable channel for forming CO/ONeMg WD – He WD and NS – He WD systems (Belczynski & Taam 2004). In fact such a channel would be very similar to the *case B* scenario but for an initially much lighter companion. For companions not massive enough to experience the He flash, a CE phase is possible if the onset of mass transfer occurs late enough in the evolution so that the companion has reached the asymptotic giant branch. In this case, the RLO becomes unstable and it bifurcates from the standard *case A* track to the CE phase.

Pulsars experiencing this evolution would be partially recycled, like *case B* systems, but they would have He WD companions. After this stage, only sufficiently tight systems with orbital periods of about one hour or less can evolve to become UCXBs within a Hubble time because gravitational decay is negligible for wider orbits. If PSR J1744–3922-like pulsars belong to the long orbital separation high-end of the UCXB formation channel, we might expect to see more such pulsars at similar and smaller orbital separations than PSR J1744–3922. It is

possible, however, that the observed sample is biased: as the orbital separation decreases, wind and mass loss by the companion become more important and would make them more difficult to detect in classical pulsar surveys conducted at low frequency (i.e. ~ 400 MHz) where eclipses are more frequent and radio emission might simply turn off. The ongoing ALFA survey at Arecibo, at 1400 MHz (Cordes et al. 2006), could therefore find several new pulsars like PSR J1744–3922. Additionally, larger orbital accelerations make them more difficult to find and, since gravitational wave radiation varies as the fourth power of the orbital separation, their lifetimes are dramatically shorter.

In such a scenario, these pulsars might be born at a spin period that is comparable with those of *case B* pulsars having CO WD companions, assuming that the short, high-accretion rate recycling would efficiently screen the magnetic field during the mass transfer process. Afterwards, because of their relatively larger magnetic field, they would spin down more rapidly than *case B* pulsars. Thus, they would necessarily have longer spin periods and the true age is more likely to be in agreement with the measured characteristic age.

5.3. AIC Channel

Finally, a third scenario to explain the unusual properties of PSR J1744–3922 is the accretion-induced collapse (AIC) of a massive ONeMg WD into a NS. Most likely AIC progenitors would be massive ONeMg WDs ($\gtrsim 1.15 M_{\odot}$) accreting from MS donors in CV-like systems, or from red giants or He WDs in UCXB systems (see Taam 2004; Ivanova & Taam 2004, for more details). Nomoto & Kondo (1991) have shown that for accretion rates $\gtrsim 0.001 \dot{M}_{Edd}$ and/or metal-rich accreted mass, the ONeMg WD would collapse to a NS rather than explode in a supernova. More recent calculations including Coulomb corrections to the equation of state by Bravo & García-Senz (1999) demonstrate that AIC is possible for critical densities of the accreting WD core that are 30% lower than previously found by Nomoto & Kondo (1991), thus facilitating the formation of neutron stars through this channel.

The properties predicted by the AIC scenario nicely agree with what we observe for the class we are proposing: the mass transfer prior to the NS formation would explain the low mass of the companion and the collapse is expected to be a quiet event during which almost no mass is lost in the system and only $\sim 0.2 M_{\odot}$ is converted in binding energy into the NS. This would keep the final orbital period close to what it was prior to the collapse (which is small in most scenarios leading to AIC) and allow the eccentricity to be very small or, at least, circularize rapidly. The survival rate of such systems is probably higher than for standard systems which are more likely to be disrupted if a large amount of mass is lost during the supernova process. Although the initial properties of pulsars formed by AIC are not known, we may presume they resemble those of “normal” pulsars with magnetic fields in the 10^{11-12} G range. Another interesting point to consider is that the AIC channel does not require a degenerate companion. As opposed to the other two proposed scenarios (Sections 5.1 and 5.2), the formation of a pulsar through AIC can interrupt the mass

transfer, thus postponing further evolution. If the “evolutionary quiescence” is long enough, we would expect to find some non-degenerate companions around young AIC pulsars having circular orbits but with spin periods and magnetic fields that are more typical of isolated pulsars. Finally, as the companion continues to evolve to fill its now larger Roche lobe, a shortened accretion phase might occur, thus transferring a very small amount of mass to the pulsar and leaving it partly recycled despite its low-mass companion.

Some binary pulsars among the group we highlighted, like PSRs B1831–00 and B1718–19, have been proposed as AIC candidates in the past (van den Heuvel & Bitzaraki 1995; Ergma 1993). However, there is no firm evidence to support this. For instance, PSR B1718–19 is presumably a member of the globular cluster NGC 6342. As Janssen & van Kerkwijk (2005) show, although observations suggest AIC is possible, an encounter and tidal capture scenario cannot be ruled out and is very reasonable given the plausible globular cluster association. On the other hand, PSR B1718–19 shares similarities with other binary pulsars in the Galactic field, especially with PSR J1744–3922. PSR B1718–19’s younger age, larger magnetic field and spin period, as well as the fact that it has a non-degenerate companion, are all compatible with it being an AIC pulsar in the intermediate “quiescent” phase.

In this context, the other pulsars of our putative class would have reached the final evolutionary stage and, hence, display mildly recycled properties. If so, PSR J1744–3922 likely has a very light He WD companion. This might explain the lack of traditional eclipses as in PSR B1718–19 (Lyne et al. 1993), large DM variations as in NGC 6397A (D’Amico et al. 2001), and orbital period derivatives as in other compact binary pulsars (Nice, Arzoumanian & Thorsett 2000) since tidal effects are important for non-degenerate companions. If the residual recycling phase left PSR J1744–3922 with a long spin period, the cooling age of its hypothetical WD companion could be smaller than the characteristic age of the pulsar for the same reason described in the recycled high magnetic field pulsar scenario (see Section 5.1). Also, pulsars forming through AIC can have lower masses than those made in standard supernovae and since they only accrete a small amount of mass from their companion afterwards, they might be less massive than conventionally formed MSPs.

6. CONCLUSIONS

This paper highlights the unusual nature of the binary pulsar system PSR J1744–3922. The puzzling radio flux modulation that it exhibits does not show typical nulling properties as displayed by some old isolated pulsars; specifically, we have found strong evidence that its variation is highly frequency dependent. Although our orbital modulation analysis does not show a significant correlation between orbital phase and flux, the modulation could still be caused by a process related to a wind from its companion, which results in short time scale variations grouped in extreme modulation “events”. Additional monitoring of both the pulsar and of its companion may prove useful in this regard.

We pointed out that this pulsar has an unusual combi-

nation of characteristics: long spin period, very low-mass companion, high magnetic field and short orbital period, that are unexplained by standard binary pulsar evolution scenarios. We propose that PSR J1744–3922, along with a several other binary pulsar systems, are part of a new class of low-mass binary pulsars which failed to be fully recycled. Specifically, we suggest three alternative scenarios for this class of binary pulsars. Distinguishing among them may be possible by improving our knowledge of the nature of their companions. We also reported the detection of a possible near-infrared counterpart to PSR J1744–3922’s companion, however, determining its nature will require detailed near-infrared/optical follow-up.

R.P.B. would like to thank Carl Bignell for his help with the GBT observations. Funding for this work was

provided by NSERC Discovery Grant Rgpin 228738-03, Fonds de Recherche de la Nature et des Technologies du Québec, the Canadian Institute for Advanced Research and Canada Foundation for Innovation. V.M.K. is a Canada Research Chair. P.B. is a Cottrell Scholar of Research Corporation. R.P.B. acknowledges the support from the Student and Postdoc Observing Travel Fund of the National Research Council of Canada’s Herzberg Institute of Astrophysics. The Green Bank Telescope is part of the National Radio Astronomy Observatory, a facility of the National Science Foundation operated under cooperative agreement by Associated Universities, Inc. The Parkes Observatory is operated by the Australia Telescope National Facility, ATNF, a division of the Commonwealth Scientific and Industrial Research Organisation, CSIRO.

REFERENCES

- Backer, D. C., 1970, *Nature*, 228, 42
 Bartel, N., et al., 1981, *A&A*, 93, 85
 Belczynski, K. & Taam, R. E., 2004, *ApJ*, 603, 690
 Bergeron, P., Saumon, D. & Wesemael, F., 1995, *ApJ*, 443, 764
 Bergeron, P., 2001, *ApJ*, 558, 369
 Bergeron, P., Leggett, S. K. & Ruiz, M. T., 2001, *ApJS*, 133, 413
 Biggs, J. D., 1992, *ApJ*, 394, 574
 Bhat, N. D. R., Gupta, Y., Kramer, M., Karastergiou, A., Lyne, A. G. & Johnston, S., 2006, *A&A*, in press
 Bravo, E. & García-Senz, D., 1999, *MNRAS*, 307, 984
 Casali, M. & Hawarden, T., 1992, *JCMT-UKIRT Newsletter*, 4, 33
 Cordes, J. M. & Rickett, B. J., 1998, *ApJ*, 507, 846
 Cordes, J. M. & Lazio, T. J. W., 2002, *astro-ph/0207156*
 Cordes, J. M., et al., 2006, *ApJ*, 637, 446
 Crawford, F., Roberts, M. S. E., Hessels, J. W. T., Ransom, S. M., Livingstone, M., Tam, C. R. & Kaspi, V. M., 2006, *ApJ*, in press
 D’Amico, N., Possenti, A., Manchester, R. N., Sarkissian, J., Lyne, A. G. & Camilo, F., 2001, *ApJ*, 561, L89
 Driebe, T., Schoenberner, D., Bloeker, T. & Herwig, F., 1999, *A&A*, 339, 123
 Drimmel, R., Cabrera-Lavers, A. & Lopez-Corredoira, M., 2003, *A&A*, 409, 205
 Edwards, R. T. & Bailes, M., 2001, *ApJ*, 553, 801
 Ergma, E., 1993, *A&A*, 273, L38
 Ergma, E., Sarna, M. J. & Giersz, M., 1996, *A&A*, 307, 768
 Faulkner, A. J., et al., 2004, *MNRAS*, 355, 147
 Fruchter, A. S., Stinebring, D. R. & Taylor, J. H., 1988, *Nature*, 333, 237
 Haslam, C. G. T., Salter, C. J., Stoffel, H. & Wilson, W. E., 1982, *A&AS*, 47, 1
 Haslam, C. G. T., Salter, C. J., Stoffel, H. & Wilson, W. E., NCSA Astronomy Digital Image Library
 Hessels, J. W. T., Ransom, S. M., Stairs, I. H., Freire, P. C. C., Kaspi, V. M. & Camilo, F., 2006, *Science*, 311, 1901
 Ibrahim, A. I., et al., 2004, *ApJ*, 609, L21
 Ivanova, N. & Taam, R. E., 2004, *ApJ*, 601, 1058
 Janssen, T., van Kerkwijk, M. H., 2005, *A&A*, 439, 433
 Kaspi, V. M., 2005, in *IAU Symposium no. 218, Young Neutron Stars and Their Environments*, ed. F. Camilo & B. M. Gaensler (San Francisco: ASP), 231
 Konar, S. & Choudhuri, A. R., 2004, *MNRAS*, 348, 661
 Li, X. & Wang, Z., 1995, *Chinese Astron. Astrophys.*, 19, 302
 Lyne, A. G., Biggs, J. D., Harrison, P. A. & Bailes, M., 1993, *Nature*, 361, 47
 Manchester, R. N., Hobbs, G. B., Teoh, A. & Hobbs, M., 2005, *AJ*, 129, 1993
 Maron, O., Kijak, J., Kramer, M. & Wielebinski, R., 2000, *A&AS*, 147, 195
 Nice, D. J., Arzoumanian, Z. & Thorsett, S. E., 2000, in *ASP Conf. Ser. 202, Pulsar Astronomy - 2000 and Beyond*, ed. M. Kramer, N. Wex & N. Wielebinski (San Francisco: ASP), 67
 Nomoto, K. & Kondo, Y., 1991, *ApJ*, 367, L19
 Payne, D. J. B. & Melatos, A., 2004, *MNRAS*, 351, 569
 Payne, D. J. B., 2005, Ph.D. Thesis, The University of Melbourne
 Phinney, E. S., 1992, *Phil. Trans. Roy. Soc. A*, 341, 39
 Ransom, S. M., Hessels, J. W. T., Stairs, I. H., Freire, P. C. C., Camilo, F., Kaspi, V. M. & Kaplan, D. L., 2005, *Science*, 307, 892
 Ransom, S. M., Roberts, M. S. E., Hessels, J. W. T., Livingstone, M., Crawford, F., Tam, C. & Kaspi, V. M., 2006, in prep.
 Rappaport, S., Podsiadlowski, P., Joss, P. C., Di Stefano, R. & Han, Z., 1995, *MNRAS*, 273, 731
 Rickett, B. J., 1970, *MNRAS*, 150, 67
 Rieke, G. H. & Lebofsky, M. J., *ApJ*, 288, 618
 Rigaut, F., et al., 1998, *PASP*, 110, 152
 Skrutskie, M. F., et al., 2006, *AJ*, 131, 1163
 Stairs, I. H., 2004, *Science*, 304, 547
 Stairs, I. H., et al., 2005, *ApJ*, 632, 1060
 Stetson, P. B., 1987, *PASP*, 99, 191
 Sutantyo W. & Li, X., 2000, *A&A*, 360, 633
 Taam, R. E., 2004, *Rev. Mexicana Astron. Astrofis.*, 20, 81
 Tauris, T. M. & Savonije, G. J., 1999, *A&A*, 350, 928
 van Den Heuvel, E. P. J. & Bitzaraki, O., 1995, *A&A*, 297, L41
 van Kerkwijk, M. H., Kaspi, V. M., Klemola, A. R., Kulkarni, S. R., Lyne, A. G., & van Buren, D., 2000, *ApJ*, 529, 428
 van Kerkwijk, M. H., Bassa, C. G., Jacoby, B. A. & Jonker, P. G., 2005, in *ASP Conf. Ser. 328, Binary Radio Pulsars*, F. A. Rasio & I. H. Stairs (San Francisco: ASP), 357
 van Paradijs, J., van den Heuvel, E. P. J., Kouveliotou, C., Fishman, G. J., Finger, M. H. & Lewin, W. H. G., 1997, *A&A*, 317, L9
 Verbunt, F., 1993, *ARA&A*, 31, 93
 Woods, P. M. & Thompson, C., 2006, *Compact Stellar X-ray Sources*, eds. W.H.G. Lewin and M. van der Klis (Cambridge University Press), 39, 547

TABLE 1
ORBITAL AND TIMING PARAMETERS FOR PSR J1744–3922^a

Parameter	Value
Orbital Period, P_{orb} (days)	0.19140635(1)
Projected Semi-Major Axis, x (lt-s)	0.21228(5)
Orbital Period Derivative, $ \dot{P}_{orb} $ (s s ⁻¹)	$< 2 \times 10^{-10}$
Projected Semi-Major Axis Derivative, $ \dot{x} $ (lt-s s ⁻¹)	$< 7 \times 10^{-12}$
Derived Parameters	
Eccentricity, e	< 0.001
Mass Function, f_1 (M_{\odot})	0.0002804(2)
Minimum Companion Mass, M_c (M_{\odot})	≥ 0.085
Surface Dipole Magnetic Field, B (G)	1.7×10^{10}
Spin Down Energy Loss Rate (erg s ⁻¹)	1.2×10^{31}
Characteristic Age, (yr)	1.7×10^9

NOTE. — Numbers in parentheses represent twice the formal errors in the least significant digits as determined by TEMPO after scaling the TOA errors such that the reduced- χ^2 of the fit was unity. The pulsar is assumed to have mass $1.4 M_{\odot}$.

^a Values reported from Ransom et al. (in prep.).

TABLE 2
DETAILS OF THE RADIO OBSERVATIONS

ν_{center} ^a MHz	BW ^b MHz	Num. chan. ^c	Sampling μ s	T_{sys} ^d K	Gain K/Jy	T ^e min	Num. obs. ^f
Parkes Telescope							
680/2900 ^g	56/576	256/192	500/500	68/31	0.625/0.59	20/20	5
1375	288	96	500	28	0.71	17	69
1400	576	192	250	32	0.71	15	13
Green Bank Telescope							
820	48	96	72	37	2.0	18	4
1400	96	96	72	24	2.0	25	19
1850	96	96	72	22	1.9	60	3
1950	600	768	81.92	22	1.9	210	4
4600	800	1024	81.92	20	1.85	257	1

NOTE. — Receiver temperatures and gains are estimated operating values. Parkes values are provided by J. Reynolds (private comm.). The system temperature corresponds to the sum of the receiver temperature and the sky temperature, which is determined from the 408 MHz all-sky survey and converted to other frequencies by assuming a power-law spectrum having a spectral index -2.6 (Haslam et al. 1982, 1995).

^a Central frequency of the receiver.

^b Observing bandwidth.

^c Number of frequency channels.

^d System temperature.

^e Average total integration time per observation.

^f Number of observations.

^g Observations were made simultaneously at these two frequencies.

TABLE 3
PERCENT OF OBSERVATIONS WITH NO DETECTION OF
PSR J1744–3922

Frequency MHz	Parkes %	GBT %	Both %
680 ^a	100 (5)	– (–)	100 (5)
820	– (–)	75 (4)	75 (4)
1400	33 (72)	32 (19)	33 (91)
1850	– (–)	0 (3)	0 (3)
1950	– (–)	0 (4)	0 (4)
2900 ^a	50 (4)	– (–)	50 (4)
4600	– (–)	0 (1)	0 (1)
Total	38 (81)	29 (31)	35 (112)

NOTE. — Numbers in parentheses represent the total number of observations for each band.

^a Observations at 680 MHz and 2900 MHz were simultaneous. Excessive RFI contamination prevents us from using one of the 2900 MHz observations.

TABLE 4
ESTIMATED PULSED FLUX DENSITY OF PSR J1744–3922

Frequency MHz	Num. data ^a	Average mJy	Standard Deviation mJy	Maximum mJy
680	40	<0.07 ^b	–	–
820	20	0.10	0.06	0.22
1400	2244	0.11	0.16	0.45
1850	142	0.11	0.04	0.20
1950	852	0.08	0.04	0.19
2900	40	0.09	0.08	0.16
4600	258	0.006	0.012	0.03

NOTE. — Pulsed flux density values were derived using the radiometer equation, implicitly assuming that the off-pulse RMS is a good estimate of the system temperature and that the sky emits according to the 408 MHz all-sky survey (Haslam et al. 1982, 1995). Relative errors are estimated to be $\sim 30\%$.

^a Number of data points used at each frequency. The time resolution is 1 minute per data point.

^b 3σ upper limit.

TABLE 5
CHARACTERISTICS OF PARTLY RECYCLED BINARY PULSARS ($P_s > 8$ MS) IN
THE GALACTIC FIELD IN LOW-ECCENTRICITY ORBITS ($e < 0.01$) AND
HAVING LOW-MASS COMPANIONS ($M_{c,min} < 0.2 M_\odot$)

Name	P ms	$\log B$ G	P_{orb} days	$M_{c,min}$ ^a M_\odot	Type
<i>Case A</i>	< 8	8-9	–	< 0.45	He WD
<i>Case B</i>	$\gtrsim 8$	9-10	–	$\gtrsim 0.45$	CO WD
PSR J1744–3922	172.44	10.22	0.19	0.08	?
PSR B1718–19 ^b	1004.03	12.11	0.25	0.12	Bloated MS ^c
PSR B1831–00	520.95	10.87	1.81	0.06	?
PSR J1232–6501	88.28	9.93	1.86	0.14	?
PSR J1614–2318	33.50	9.14	3.15	0.08	?
PSR J1745–0952	19.37	9.51	4.94	0.11	?
PSR B1800–27	334.41	10.88	406.78	0.14	?
PSR J0407+1607	25.70	9.16	669.07	0.19	?

^a $M_{c,min}$ refers to the minimum mass of the companion corresponding to an orbital inclination angle of 90° and assuming a mass for the pulsar of $1.35 M_\odot$.

^b In globular cluster NGC 6342.

^c Janssen & van Kerkwijk (2005)

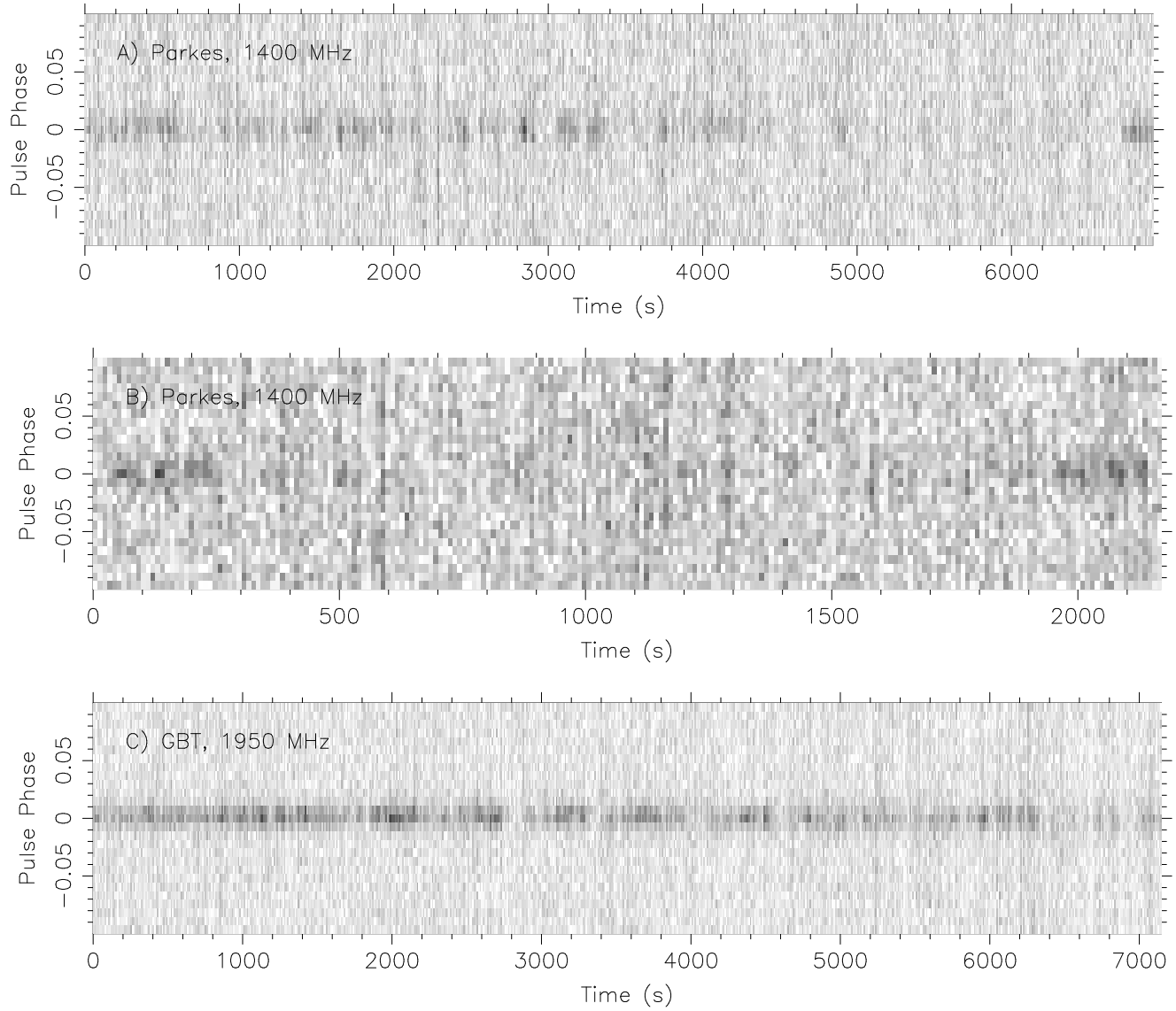


FIG. 1.— Sample folded intensity profiles of PSR J1744–3922 as a function of time for two 1400 MHz observations at Parkes with 576 MHz bandwidth (panel A & B) and a 1950 MHz observation at GBT with 600 MHz bandwidth (panel C). The grayscale represents the intensity of the signal, with darker regions being brighter. The center of the gaussian-like pulse profile should appear at the pulse phase = 0.

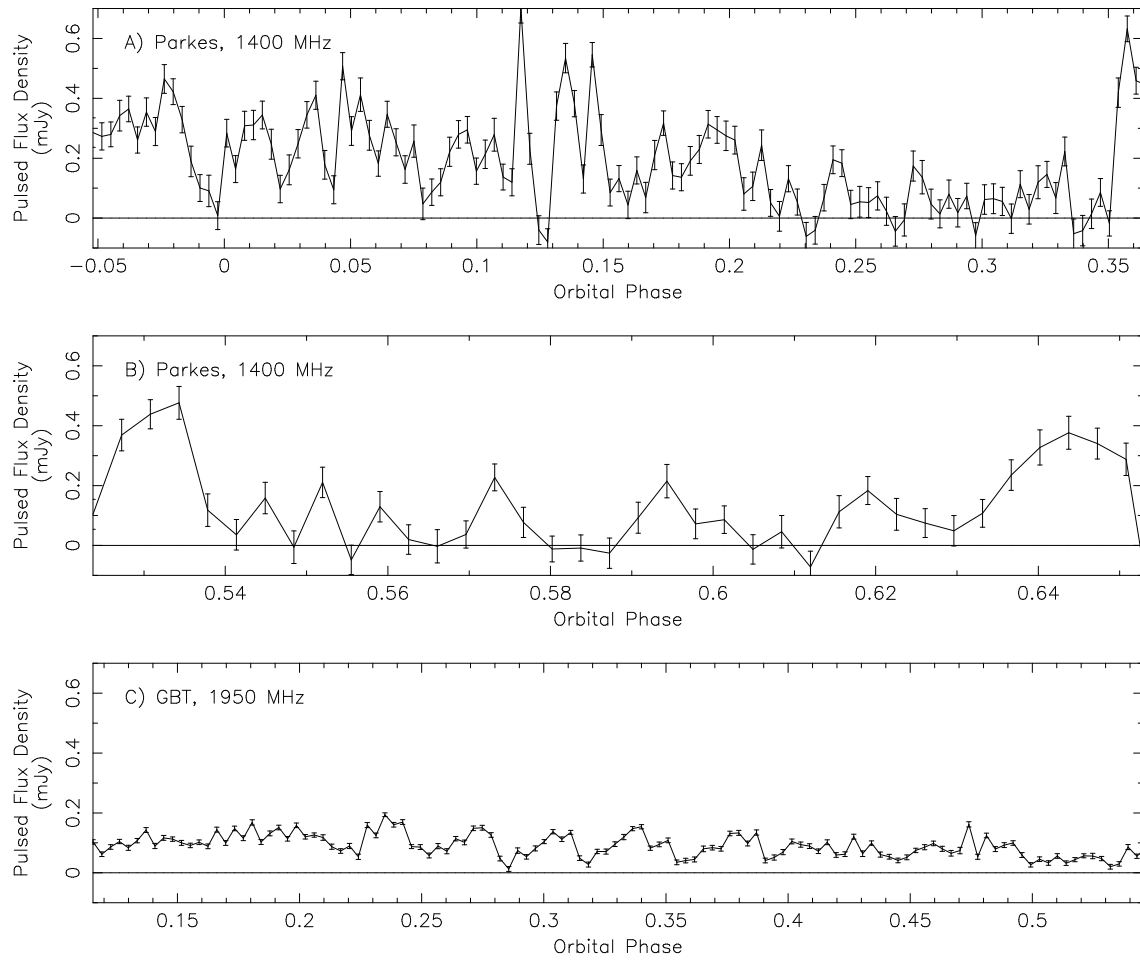


FIG. 2.— Sample light curves of the pulsed radio flux density as a function of orbital phase. Each data point represents 60 sec of data and orbital phases are defined so that 0.25 is when the companion is in front of the pulsar. Panel A, B and C are the two 1400 MHz observations and the 1950 MHz observation, respectively, displayed in Figure 1. We note that the flux drops below the detection limit at 1400 MHz several times whereas it appears to be always above this threshold at 1950 MHz. Also, as illustrated in Figure 3, the variability is much stronger at lower frequency.

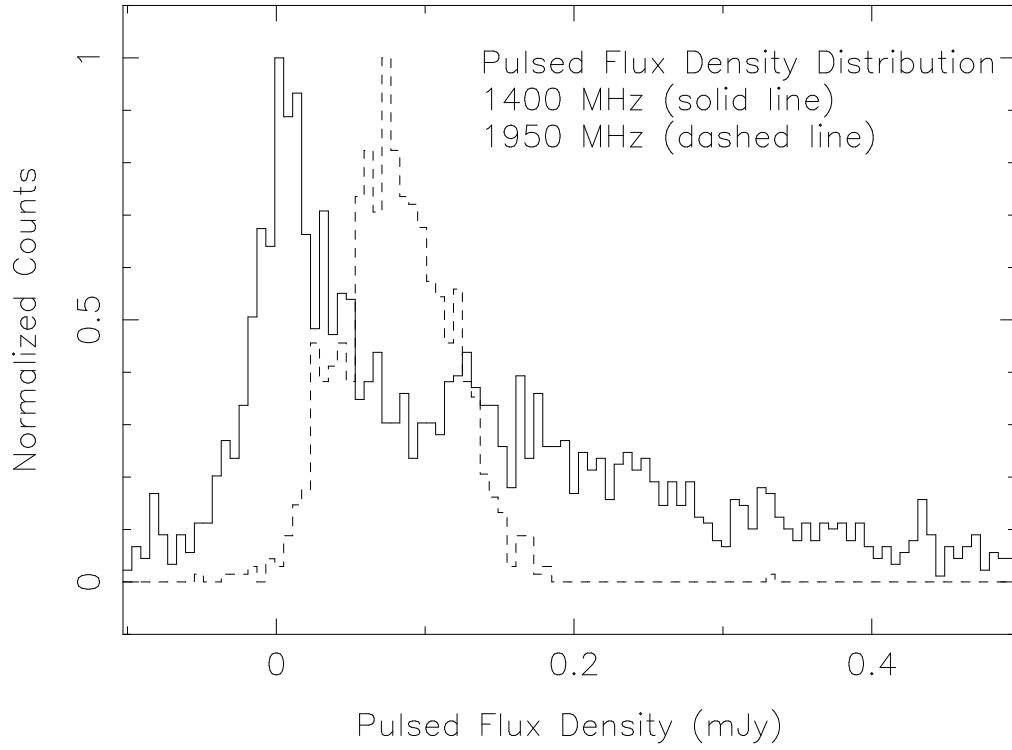


FIG. 3.— Distribution of the measured pulsed flux density values at 1400 MHz (solid line) and at 1950 MHz (dashed line). The 3σ sensitivity threshold is ~ 0.02 and 0.01 mJy at 1400 and 1950 MHz, respectively. We observe that PSR J1744–3922 rarely disappears at 1950 MHz whereas there is a significant number of non-detections, centered about zero, at 1400 MHz (negative values are reported when the pulsed flux density is below the telescope sensitivity, meaning the flux determination algorithm has fit noise). Also, we note that the pulsed flux density is more variable and spans over higher values at 1400 MHz than at 1950 MHz.

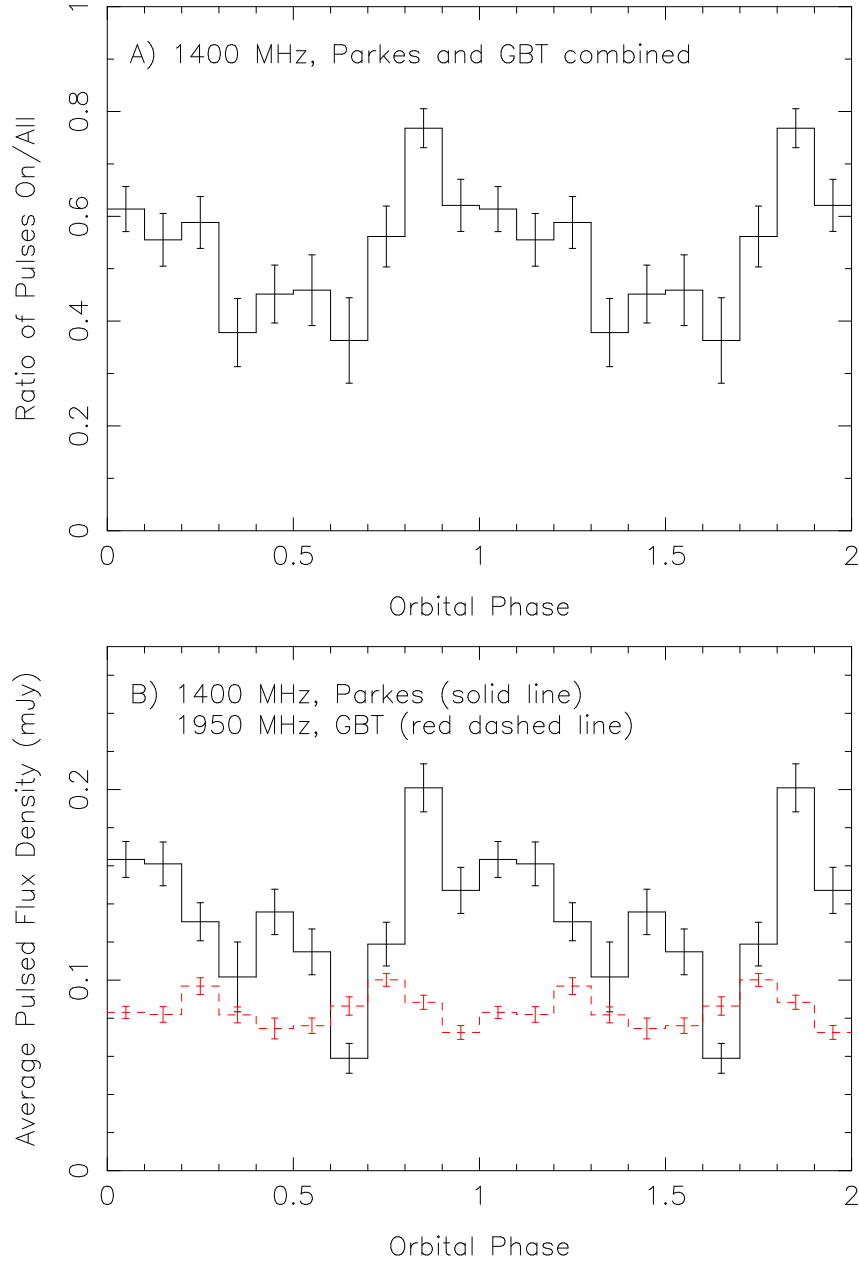


FIG. 4.— Ratio of pulses detected with respect to the total number observed at different orbital phases for the 1400 MHz Parkes and GBT combined (panel A) and a similar plot showing the average pulsed flux intensity (panel B) for the Parkes 1400 MHz data (solid line) and the GBT 1950 MHz data (red dashed line). Orbital phases are defined so that 0.25 is the pulsar’s superior conjunction (i.e. the companion passes in front of the pulsar). The scale of the error bars represents the estimated errors without scaling from the results of the Monte Carlo simulations, hence they are likely underestimated.

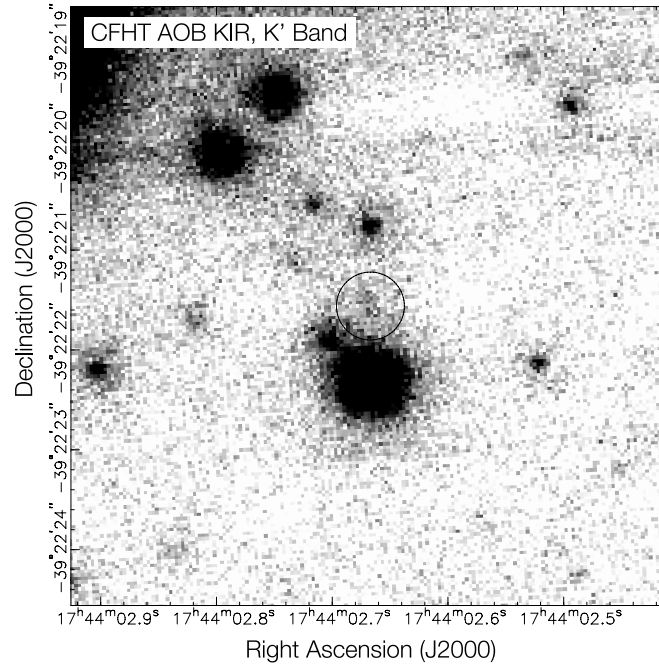


FIG. 5.— Near-infrared image of the field of PSR J1744–3922 in the K' band, obtained with AOB KIR at CFHT. The $0''.34$ positional error circle (3σ confidence) is shown, with the proposed counterpart at the centre.

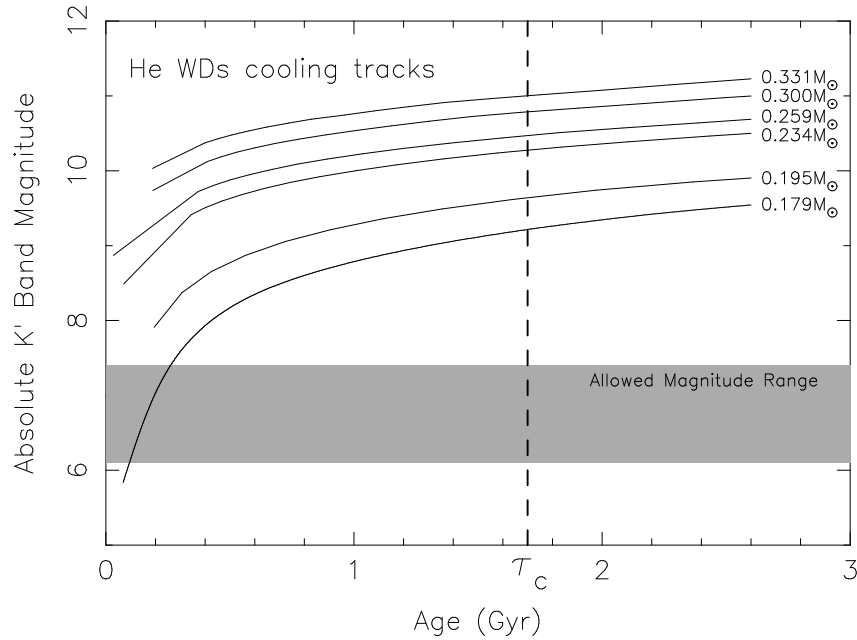


FIG. 6.— Cooling tracks for He WDs made using the evolution sequences of Driebe et al. (1999) and our atmosphere models (see Bergeron et al. 1995, 2001; Bergeron 2001, for more details). Lines show the cooling for constant masses of 0.179, 0.195, 0.234, 0.259, 0.300 and 0.331 M_{\odot} , from bottom to top, respectively. The shaded region is the restricted range of absolute K' band magnitude inferred from the CFHT data, and the dotted vertical line indicates the characteristic age of PSR J1744–3922.

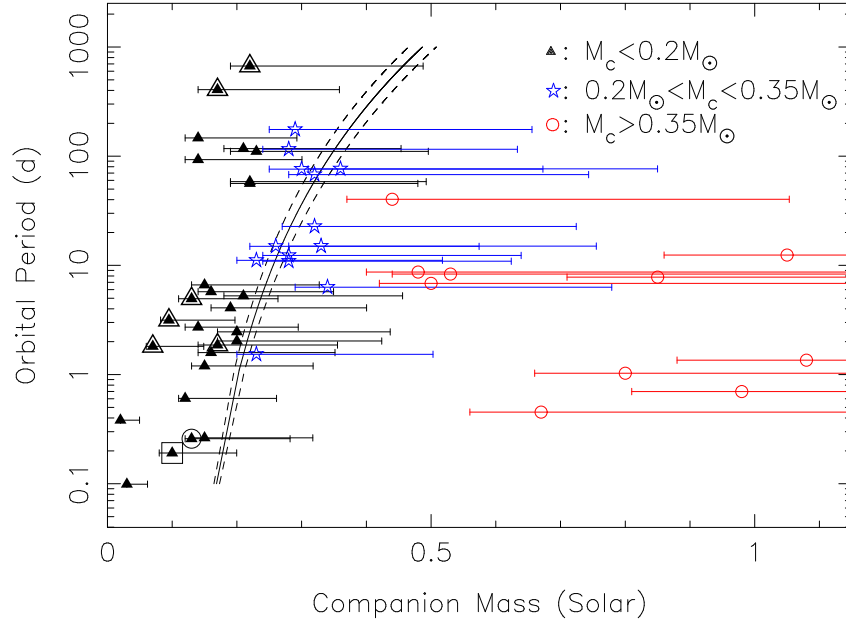


FIG. 7.— Orbital period versus companion mass for binary pulsars in the Galactic field in circular orbits ($e < 0.01$). Symbols indicate the companion median mass (corresponding to $i = 60^\circ$) and are coded according to the minimum mass: $M_c \leq 0.2 M_\odot$, $0.2 M_\odot < M_c \leq 0.35 M_\odot$ and $M_c > 0.35 M_\odot$ are black triangles, blue stars and red circles, respectively. Error bars cover the 90 %-probability mass range for randomly oriented orbits having $i = 90^\circ$ to $i = 26^\circ$. The curves are the predicted $P_{orb} - M_c$ relationships for different metallicity progenitors (from Tauris & Savonije 1999). PSR J1744–3922 is identified by a square outline and pulsars listed in Table 5 with triangle outlines. The plot also includes the globular cluster pulsar PSR B1718–19 (marked by a circle outline) because it resembles PSR J1744–3922 (see Section 2.4). Data from the ATNF Pulsar Catalogue (Manchester et al. 2005) (<http://www.atnf.csiro.au/research/pulsar/psrcat/>).

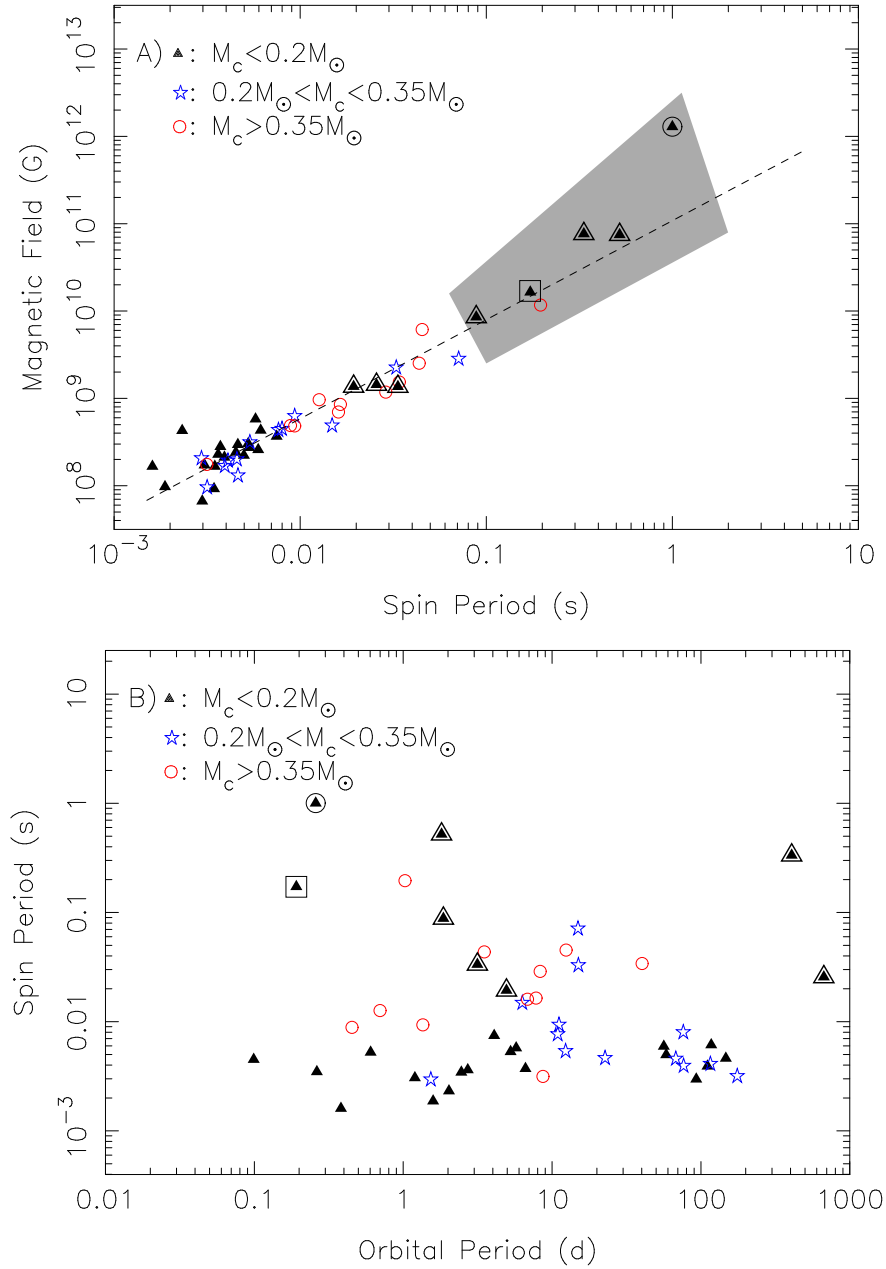


FIG. 8.— Inferred surface dipolar magnetic field strength versus spin period (panel A) and spin period versus orbital period (panel B) for binary pulsars in the Galactic field in circular orbits ($e < 0.01$). Symbols are coded according to the companion minimum mass: $M_c \leq 0.2 M_\odot$, $0.2 M_\odot < M_c \leq 0.35 M_\odot$ and $M_c > 0.35 M_\odot$ are black triangles, blue stars and red circles, respectively. PSR J1744-3922 is identified by a square outline and pulsars listed in Table 5 with triangle outlines. The shaded area is the approximate region where is the proposed class of binary pulsars similar to PSR J1744-3922. The plots also include the globular cluster pulsar PSR B1718-19 (marked by a circle outline) because it resembles PSR J1744-3922 (see Section 2.4). The dashed line is the best-fit for a power-law, $B \propto P^\alpha$, with $\alpha = 1.13$. We excluded PSR B1718-19 from the fit as it is in a globular cluster. Data from the ATNF Pulsar Catalogue (Manchester et al. 2005) (<http://www.atnf.csiro.au/research/pulsar/psrcat/>).